PRESSURE DROP AND STABILITY OF FLOW IN ARCHIMEDEAN SPIRAL TUBE WITH TRANSVERSE CORRUGATIONS

by

Milan Lj. DJORDJEVIĆ[a]*, Velimir P. STEFANOVIĆ[b], and Marko V. MANČIĆ[b]

[a] Faculty of Technical Sciences, University of Pristina, Kosovska Mitrovica, Serbia
[b] Faculty of Mechanical Engineering, University of Nis, Nis, Serbia

Original scientific paper
DOI: 10.2298/TSCI150118212D

Isothermal pressure drop experiments were carried out for the steady Newtonian fluid flow in Archimedean spiral tube with transverse corrugations. Pressure drop correlations and stability criteria for distinguishing the flow regimes have been obtained in a continuous Reynolds number range from 150-15000. The characterizing geometrical groups which take into account all the geometrical parameters of Archimedean spiral and corrugated pipe has been acquired. Before performing experiments over the Archimedean spiral, the corrugated straight pipe having high relative roughness e/d = 0.129 of approximately sinusoidal type was tested in order to obtain correlations for the Darcy friction factor. Insight into the magnitude of pressure loss in the proposed geometry of spiral solar receiver for different flow rates is important because of its effect upon the efficiency of the receiver. Although flow in spiral and corrugated geometries has the advantages of compactness and high heat transfer rates, the disadvantage of greater pressure drops makes hydrodynamic studies relevant.

Key words: *Archimedean spiral tubes, transverse corrugated pipes, pressure drop*

Introduction

Significant effort has been made to advance heat transfer enhancement techniques in order to improve the overall performance of heat exchangers. Flow through curved channel geometries has advantages over the conventional straight channel under certain situations and applications. The presence of superimposed secondary flows in curved channel flow causes various substantial features, such as: (a) the increased heat and mass transfer coefficients due to cross-sectional mixing of fluid elements, (b) secondary convection suppresses the axial propagation of initial turbulent fluctuations, so that the curvature stabilizes the flow and transition from laminar to turbulent flow is delayed, and (c) frictional losses in the fluid stream are enhanced.

Most of the hydrodynamic studies on the coil flows have been dedicated to the helical coils. Much less work has been reported for the hydrodynamics of flow through spiral coils. The property of continuously varying curvature along the length makes spiral coil flows never fully developed, unlike the helical coil flows. Secondly, the distinction of flow regime needs specification of two critical Reynolds numbers instead of just one [1]. In a spiral coil completely filled with laminar flow slow increase of Reynolds number causes the appearance

* Corresponding author; e-mail: milan.djordjevic@pr.ac.rs

of the turbulent flow zone at the outer end at the approach of the first critical Reynolds number. Further increase of Reynolds number extends turbulent flow zone toward the inner end of the coil until it completely fills the coil with turbulent flow at the second critical Reynolds number. Moreover, there is a possibility of existence of mixed flow inside the spiral coil, where some length of the coil being in the laminar flow and some other length in the turbulent flow. Consequently, the phenomena of the forward and the reverse laminar-turbulent transition can occur in the spiral coil.

Naphon and Wongwises [2] have reviewed the literature for three main categories of curved tubes: helically coiled tubes, spirally coiled tubes, and others curved tube arrangements. They concluded that there are very few published studies on the spiral coils where the curvature ratio variation (d/D_c) is below 0.1, where d is tube diameter and D_c is the diameter of curvature. Naphon and Wongwises [3] experimentally studied hydrodynamic characteristics of spiral coils having curvature ratio (d/D_c) variation of 0.067-0.24, and compared obtained results with helical coils. Naphon and Suwagrai [4] studied experimentally and numerically effect of curvature ratios on the heat transfer and flow development in the spirally coiled tubes. They stated that the Nusselt number and pressure drop obtained from the spirally coiled tube are 1.49 and 1.50 times higher than those from the straight tube, respectively, under constant wall temperature boundary condition.

Yoo *et al.* [5] numerically studied spiral coils of six turns with exponentially increasing radius of curvature with the polar angle. They concluded that the effect of Reynolds number was stronger than that of the curvature. Bowman and Park [6] numerically investigated laminar flow pressure drop and heat transfer characteristics of coiled systems. They have found that up to 10% of the additional pressure drop and 40% of the enhanced heat transfer characteristics were obtained from the spiral coil system over the toroidal. Altac and Altun [7] investigated numerically the convection heat transfer and the laminar friction losses in combined entry region of horizontal spiral tube coils. They summarized that the friction factor increases with the spiral tube length. However, for spiral coils of more than four turns or spiral coils of sufficient length, the normalized friction factor decreases. The normalized friction factor increases by as much as 2.5 times for coils of small radius of curvatures.

All studies cited above evaluate hydrodynamic behavior in smooth curved tubes, and no study examining spiral coil flow in rough pipes has been found in the open literature.

Tube side heat transfer enhancement techniques can be classified according to the following criteria: (a) incorporation of additional devices into a plain round tube (twisted tapes, wire coils) and (b) surface modification of a plain tube (corrugated, dimpled, and internally finned tubes). Transversal corrugations act as turbulence promoters, since flow turbulence level is increased by a separation and reattachment mechanism. Besides, corrugations act as roughness elements and disturb the existing laminar sublayer.

Perry *et al.* [8] studied the turbulent boundary layer over a wall roughened by transverse ribs and proposed dividing the roughness into two types, *d type* and *k type*, according to the significant length scale involved in determining the roughness function, velocity profiles and friction factor (k being the roughness height and d being the pipe diameter). Tani [9] suggested that for roughness consisting of regularly spaced ribs, a borderline between the *d type* and *k type* roughness might be drawn at about $p/k = 5$, where p is the pitch between contiguous roughness elements. On a *d type* rough wall, typified by closely spaced span wise ribs with p/k less than 5, vortices are setup in the grooves and eddy shedding from the elements into the flow will be negligible, and the outer flow is relatively undisturbed by the roughness elements. The friction factor and the roughness function are independent of the size of the

roughness element, but the drag on the roughness elements is extremely sensitive to vertical misalignment of the element crests. Jaiman *et al.* [10] and Pisarenko *et al.* [11] numerically investigated transversely corrugated pipes, but investigations were limited to pipes of large internal diameter, d, having low relative roughness e/d. Vijiapurapu and Cui [12] simulated the turbulent flow in a ribbed pipe using large eddy simulation and concluded that no valid relation between friction factor, equivalent sand grain roughness, ε, and corrugation depth, e, can be established from the results obtained. Bernhard and Hsieh [13] investigated two corrugated plastic pipes using water in the Re = 10^4-$2.5 \cdot 10^5$ range, and found that at the Reynolds number below $4 \cdot 10^4$ the friction factor stays nearly constant, and above it starts to rise. They suggested that the increase of the friction factor at large Reynolds numbers was caused by penetration of the flow from the core region into the corrugation recesses. Taylor *at al*. [14] reviewed effects of surface roughness and texture on fluid flow, with special reference to structured roughness surfaces. They concluded that in order to develop accurate friction factor predictive models, experimental data is needed in the laminar, transition and turbulent flow with uniform relative surface roughness values beyond 0.05.

From the cited papers can be concluded that there is a lack of data concerning friction factor for a range of geometrical parameters and Reynolds number for transversely corrugated straight pipes having large relative roughness, e/d. Moreover, no reference concerning hydrodynamic in spiral tube coils with transverse corrugations was found.

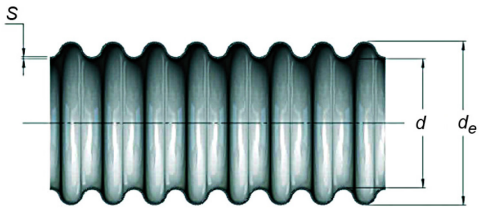

Figure 1. Profile of transverse corrugated pipe

Experimental

The measurements of pressure losses in developed laminar, transition, and turbulent region of transversely corrugated straight pipe and Archimedean spiral coil flow were described. The commercially available stainless steel pipes [15] shown in fig. 1 were tested in the range of Re = 150-15000.

The geometrical characteristics and experimental configurations of transversely corrugated straight pipe and transversely corrugated Archimedean spiral coil are shown in figs. 2 and 3, respectively, while tab. 1 shows geometrical parameters of tested configurations.

The tap water was used as a working fluid. Water was fed from a buffer tank by pump flow trough TA-STAD balancing valve. Water flow rate was measured with the precise volumetric flask having a resolution of 10 ml and a stopwatch. The pressure drop measurements were made by connecting the pressure taps (PT) to the water (for pressure drops up to 20 kPa) and mercury hydrostatic manometer (for pressure

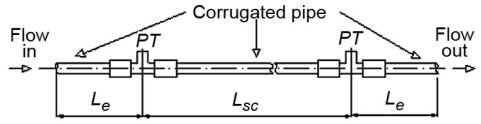

Figure 2. Geometry and configuration of transversely corrugated straight pipe

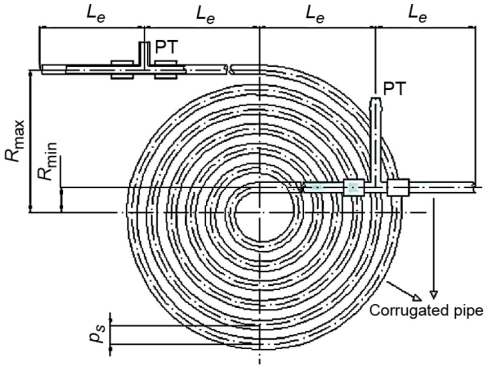

Figure 3. Geometry and configuration of transversely corrugated Archimedean spiral coil

Table 1. Geometrical parameters of tested configurations

Transversely corrugated straight pipe				Transversely corrugated Archimedean spiral coil			
d	9.3	[mm]	minimum internal diameter	d	9.3	[mm]	minimum internal diameter
d_0	11.7	[mm]	maximum internal diameter	d_0	11.7	[mm]	maximum internal diameter
d_e	12.2	[mm]	maximum external diameter	d_e	12.2	[mm]	maximum external diameter
S	0.25	[mm]	wall thickness	e	1.2	[mm]	corrugation depth
e	1.2	[mm]	corrugation depth	e/d	0.1290	[–]	relative roughness
e/d	0.1290	[–]	relative roughness	p_c	4.2	[mm]	corrugation pitch
p_c	4.2	[mm]	corrugation pitch	p_s	13.6	[mm]	spiral coil pitch
L_{sc}	2	[m]	length of tested section	L_{scc}	9.324	[m]	length of the coil
L_e	0.5	[m]	length of entrance section	L_e	0.5	[m]	length of entrance section
				R_{min}	25	[mm]	minimum radius of the coil
				R_{max}	202	[mm]	maximum radius of the coil
				n	13	[–]	number of coil turns

drops higher than 20 kPa). In both experimental set-ups, the lengths of straight tubing of the entrance and exit sections before and after PT, were corrugated pipes of the same length, L_e, and longer than required to obtain a fully developed flow prior to entering the test sections (having lengths L_{sc} and L_{scc}). In the case of spiral coil there were additional lengths of straight tubing L_e to the PT (fig. 3). The measured pressure drops owing to these lengths were subtracted from each run at each Reynolds number to give only the pressure drops owing to the coiled part. The spiral was fed through the innermost and outermost turn for the full flow rate range in order to assess the uniqueness of hydrodynamics. All measurements were repeated three times and mean values used.

Properties of water were determined from the approximating formulas based on the IAPWS formulation 1995 for the thermodynamic properties of ordinary water substance for general and scientific use [16]:

– density

$$\rho(t) = 1001.1 - 0.0867t - 0.0035t^2 \tag{1}$$

– dynamic viscosity

$$\mu(T) = 1.684\cdot10^{-3} - 4.264\cdot10^{-5}T + 5.062\cdot10^{-7}T^2 - 2.244\cdot10^{-9}T^3 \tag{2}$$

The uncertainty of the measurements of friction factor were calculated according to Kline and McClintock [17] method. It varies from about 4% at high Reynolds numbers to about 8% at low Reynolds numbers. The uncertainty of measurements of low pressure drop was the primary source of the uncertainty of the friction factor at low Reynolds numbers.

Results and discussion

Transversely corrugated straight pipe

The transversal axisymmetric corrugations of the pipe under the study belong to the pipes having regular roughness of sinusoidal or *U type* [18]. The main geometrical parameters

characterizing the transversely corrugated pipes are: minimum internal diameter d, maximum internal diameter d_o, corrugation depth $e = (d_o - d)/2$, and corrugation pitch p_c.

Isothermal pressure drop experiments were carried out by employing water in order to determine Darcy friction factor, f, for corrugated straight pipe by the formula of Darcy--Weisbach:

$$\Delta p = f \frac{L_{sc}}{d} \frac{\rho V^2}{2} \tag{3}$$

where L_{sc} is the length of the pipe, V – the mean axial velocity, and ρ – the density of fluid. The loss coefficient, K, due to surface friction (analogous to the loss coefficient due to local loss) is expressed:

$$K_{sc} = f \frac{L_{sc}}{d} \tag{4}$$

The minimum internal diameter of the corrugated pipe d is used in the data reduction as the characteristic length to evaluate the $\mathrm{Re} = Vd\rho/\mu$ and friction factor f. This is in accordance with the assumption of boundary-layer flow on a *d type* rough wall [8]. Kandlikar *et al.* [19] considered the effect of flow constriction due to roughness elements and suggested that the constricted flow diameter (minimum diameter) should be taken in the Reynolds number and the friction factors calculations.

Grouping the variables of the Reynolds number in the Hagen-Poiseuille law and grouping the remaining variables as in Darcy-Weisbach's equation yields the following formula for laminar friction factor:

$$f = \frac{64}{\mathrm{Re}} \tag{5}$$

Colebrook [20] proposed an empirical implicit combination of the Prandtl and von Karman formulas that modeled very accurately artificially roughened pipes with non-uniform sand grains and duplicated very well the behavior of commercial pipes:

$$\frac{1}{\sqrt{f}} = -2 \log_{10} \left(\frac{e}{3.7 d_0} + \frac{2.51}{\mathrm{Re}\sqrt{f}} \right) \tag{6}$$

A composite plot of all regions of interest for presentation of the friction factor in a suitable form for engineering use was developed by Moody [21], and this diagram demonstrated applicability of the Colebrook-White equation over a wide range of Reynolds numbers and relative roughness. The highest value of relative roughness covered by Colebrook-White equation and the Moody diagram is 0.05, and their applicability to the higher relative roughness values cannot be ascertained.

Great number of implicit and explicit correlations evaluate the single-phase friction factor against the Nikuradse equation and the Colebrook equation, but it still remains an issue to examine similarities and differences between them to avoid misusing [22]. However, their applications are limited to the maximum value of relative roughness of 0.05.

Correlations proposed in literature covering all flow regimes (laminar, critical, transition, and fully turbulent) and any relative roughness are:

– Churchill's formula [23]

$$f = 8\left[\left(\frac{8}{\mathrm{Re}}\right)^{12} + \frac{1}{(A+B)^{\frac{3}{2}}}\right]^{1/12}, \quad \text{where } A = \left[2.457 \ln \frac{1}{\left(\frac{7}{\mathrm{Re}}\right)^{0.9} + \frac{0.27e}{d_0}}\right]^{16} \quad (7)$$

$$\text{and } B = \left(\frac{37530}{\mathrm{Re}}\right)^{16}$$

– Modified Churchill's formula [24]

$$f = \left[\left(\frac{64}{\mathrm{Re}}\right)^{12} + \frac{1}{(A+B)^{3/2}}\right]^{1/12}, \quad A = \left[0.8687 \ln \frac{1}{\frac{0.883(\ln \mathrm{Re})^{1.282}}{\mathrm{Re}^{1.007}} + \frac{0.27e}{d_0} - \frac{110e}{\mathrm{Re}\, d_0}}\right]^{16}, \quad (8)$$

$$B = \left(\frac{13269}{\mathrm{Re}}\right)^{16}$$

– Chen [25]

$$\frac{1}{\sqrt{f}} = -2 \log\left\{\frac{e}{3.7065\, d_0} - \frac{5.0452}{\mathrm{Re}} \log\left[\frac{1}{2.8257}\left(\frac{e}{d_0}\right)^{1.1098} + \frac{5.8506}{\mathrm{Re}^{0.8981}}\right]\right\} \quad (9)$$

Previously cited correlations failed to represent our experimental data, what is shown on fig 4. These correlations have close trends to Colebrook-White equation, and over predict value of friction factor in all flow regimes, even though in the fully rough.

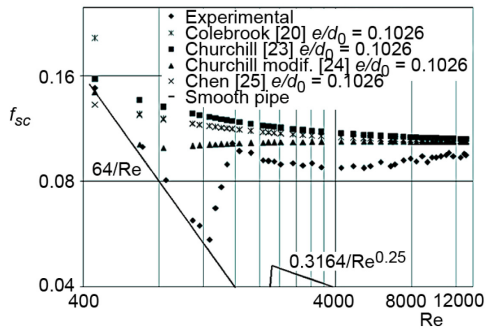

Figure 4. Friction factor *vs.* Reynolds number for tested corrugated straight pipe

Experimental data (fig. 4) show that the friction factor follows the Hagen-Poiseuille law up to the critical Reynolds number, then rise abruptly at the critical zone, followed it down for a range of Reynolds numbers in transition zone, then rise up again to meet the friction factor for turbulent flow in fully rough zone. This inflectional behavior in the transition zone is not characteristic for commercial pipes that represent model of non-uniform sand grains roughness of Colebrook [20]. On the other hand, experimental data for the corrugated pipe duplicates very well value trends of Nikuradse's results for artificially roughened pipes with uniform sand-grains. Inflection in the transition zone could be explained with the Prandtl's boundary layer theory, which states that there is always a laminar flow boundary layer that thins as Reynolds number increases. Laminar flow breaks up into a turbulent core and a laminar boundary layer next to the pipe wall in the critical zone. The elements of uniform roughness in corrugated pipes remain submerged in

the boundary layer and are hidden to the turbulent core flow. The friction factor in critical zone has close rising trend to that in smooth pipe. Further increase of Reynolds number causes the boundary layer thinning until the corrugations begin to emerge, what in turn shifts the friction factor from the smooth pipe behavior to the rough pipe behavior. Discussion regarding the onset of rough-wall behavior needs to consider the transitional properties for a particular rough surface, since it depends critically on the geometric nature of the roughness.

For examined corrugated straight pipe the characteristic flow zones were defined: laminar when Re < 1300, critical when 1300 < Re < 1600, transition 1600 < Re < 4000, and rough (turbulent) when 4000 < Re (fig. 4).

Experimental values of friction factor were correlated *vs.* Reynolds number for characteristic flow regimes and following equations were acquired:

– laminar zone

$$f_{\mathrm{sc}} = \frac{64}{\mathrm{Re}} \tag{10}$$

– critical zone

$$f_{\mathrm{sc}} = 0.0045\, e^{0.002\,\mathrm{Re}} \tag{11}$$

– transition zone

$$f_{\mathrm{sc}} = 0.0942\,(6\cdot 10^{-9}\,\mathrm{Re}^2 - 6\cdot 10^{-5}\,\mathrm{Re} + 1.081) \tag{12}$$

– rough zone

$$f_{\mathrm{sc}} = 0.0942 \tag{13}$$

The maximum absolute deviations of the obtained least-square predictions are 7% in the laminar, 4% in the critical, 5% in the transition, and 3% in the turbulent flow region.

Transversely corrugated Archimedean spiral coil

The radius of curvature is not constant and a constant pitch, p_{s}, between any two spiral turns is always assured. The Darcy friction factor and loss coefficient are defined as for a straight tube, eqs. (3) and (4), although eq. (3) is questionable on theoretical grounds when applied to developing flow.

Published work on the hydrodynamics of flow through constant pitch spiral tube coils is scarce. Existing correlations are valid for smooth tubes only and they are not applicable to rough pipes. The referent correlations for friction factor in engineering practice are proposed by Kubair and Kuloor [26]:

$$f_{\mathrm{scs}} = 50.96\left(\frac{d^2}{L_{\mathrm{scs}} D_{\mathrm{av}}}\right)^{0.3} \mathrm{Re}^{-0.5}, \qquad 300 < \mathrm{Re} < 7000 \tag{14}$$

$$f_{\mathrm{scs}} = 0.316\,\mathrm{Re}^{-0.25} + 0.41\left(\frac{d}{D_{\mathrm{av}}}\right)^{0.9}, \qquad \mathrm{Re} > 7000 \tag{15}$$

where d is inside tube diameter, D_{av} – the average coil diameter, and L_{scs} – the length of smooth spiral coil. Those equations are neither complete nor unique, since they use the arithmetic average of the innermost and outermost diameters that could be the same for geometri-

cally different coils. To specify uniquely the spiral coil, except the inside tube diameter d, three of the following variables are necessary: the maximum radius, the minimum radius, the number of turns n, the length of the coil, L, and/or distance between two consecutive turns of the coil, p_s. These parameters are shown in fig. 3.

The use of friction factor in correlations is inappropriate since the spiral flow is never fully developed and the magnitude of the pressure drop per unit length is not independent of the position along the axial length. It is expected that the pressure drop per unit length of the coil will be more in the inner turns than in the outer turns. Finally, secondary flows in a spiral coil hinder the use of static PT in the curved regions and the data based on observations of Kubair and Kuloor [26] could contain unknown errors.

Rennels and Hudson [27] proposed correlation for loss coefficient that contains all previously mentioned parametars:

$$K_{\mathrm{scs}} = \frac{R_{\max} - R_{\min}}{p_s}\left[f_{\mathrm{ss}}\pi\left(\frac{R_{\max} + R_{\min}}{d}\right) + 0.20 + 4.8 f_{\mathrm{ss}}\right] + \frac{13.2 f_{\mathrm{ss}}}{\left(\frac{R_{\min}}{d}\right)^2} \tag{16}$$

where f_{ss} is the friction factor for straight pipe, and $R_{\max}$ and $R_{\min}$ are maximum and minimum spiral coil radii, respectively. Although this correlation takes into account the friction factor, results obtained substituting the values of friction factor for straight corrugated pipe, eqs. (10)-(13), significantly mismatch even the value trends of experimental data.

Accounting for the effects of all geometrical parameters of the Archimedean spiral coils, Ali and Seshadri [1] have correlated their pressure drop experimental data:

– laminar flow (Re < 6000)

$$\frac{\Delta P_{\mathrm{scs}}}{2\rho V^2}\left[\frac{p_{\mathrm{s}} d^{1/2}}{R_{\max}^{3/4}(R_{\max} - R_{\min})^{3/4}}\right] = 49\left(\frac{dV\rho}{\mu}\right)^{-0.67} \tag{17}$$

– turbulent flow (Re > 10000)

$$\frac{\Delta P_{\mathrm{scs}}}{2\rho V^2}\left[\frac{p_{\mathrm{s}} d^{1/2}}{R_{\max}^{3/4}(R_{\max} - R_{\min})^{3/4}}\right] = 0.65\left(\frac{dV\rho}{\mu}\right)^{-0.18} \tag{18}$$

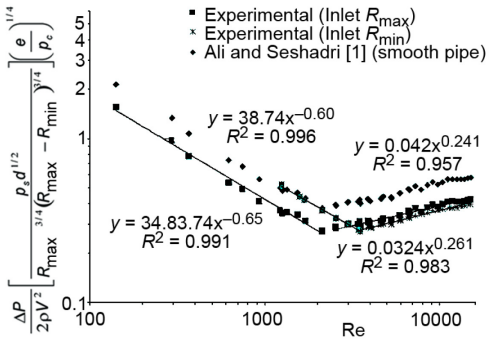

Figure 5. Generalized pressure drop correlations for transversely corrugated Archimedean spiral tube coil

Those correlations were obtained for smooth spiral coils and, as expected, mismatch our experimental data (fig. 5). In order to correlate pressure, drop experimental data for transversely corrugated Archimedean spiral coil, the geometric group given in eqs. (17) and (18) was amended with geometric parameters that define corrugated pipe – corrugation depth e and corrugation pitch p_c. Product of the half of the Euler number (Eu = $\Delta P/\rho V^2$) and newly proposed geometric group was plotted *vs.* Reynolds number on log-log paper (fig. 5).

Each experimental data graph, whether it represents inflow to outermost or innermost

spiral turn, has a sharp break giving two lines for the two main flow regimes. The best fit lines obtained by least squares analysis of the points are:

Inflow to outermost spiral turn:

– laminar flow (Re < 2100)

$$\frac{\Delta P_{\mathrm{scs}}}{2\rho V^2}\left[\frac{p_{\mathrm{s}} d^{1/2}\left(\frac{e}{p_{\mathrm{c}}}\right)^{1/4}}{R_{\max}^{3/4}(R_{\max}-R_{\min})^{3/4}}\right]=34.83\left(\frac{dV\rho}{\mu}\right)^{-0.63} \tag{19}$$

– turbulent flow (2100 < Re < 15000)

$$\frac{\Delta P_{\mathrm{scs}}}{2\rho V^2}\left[\frac{p_{\mathrm{s}} d^{1/2}\left(\frac{e}{p_{c}}\right)^{1/4}}{R_{\max}^{3/4}(R_{\max}-R_{\min})^{3/4}}\right]=0.042\left(\frac{dV\rho}{\mu}\right)^{0.241} \tag{20}$$

Inflow to innermost spiral turn

– laminar flow (Re < 3500):

$$\frac{\Delta P_{\mathrm{scs}}}{2\rho V^2}\left[\frac{p_{\mathrm{s}} d^{1/2}\left(\frac{e}{p_{c}}\right)^{1/4}}{R_{\max}^{3/4}(R_{\max}-R_{\min})^{3/4}}\right]=38.74\left(\frac{dV\rho}{\mu}\right)^{-0.6} \tag{21}$$

– turbulent flow (3500 < Re < 15000)

$$\frac{\Delta P_{\mathrm{scs}}}{2\rho V^2}\left[\frac{p_{\mathrm{s}} d^{1/2}\left(\frac{e}{p_{c}}\right)^{1/4}}{R_{\max}^{3/4}(R_{\max}-R_{\min})^{3/4}}\right]=0.032\left(\frac{dV\rho}{\mu}\right)^{0.261} \tag{22}$$

The maximum deviation of the predictions in the laminar flow region is 7% and that in the turbulent flow region is 5%.

Stability criteria

The critical Reynolds numbers for both inflow cases can be located in fig. 5 as the break points on the straight correlation lines. It is obvious that critical Reynolds number is not only a function of the geometrical parameters of a spiral, but also depends on the direction of fluid flow. When fluid enters the coil from outside, the initial straight tube turbulence in the feed line gets damped out in the inner turns as the intensity of secondary circulation increases and only one transition takes place. In the other case, when fluid enters the coil from inside, the initial straight-tube turbulence in the feed line is damped out in the innermost turns and, as the intensity of secondary circulation decreases in the outer turns, forward transition takes place. This indicat-

ing that transition lengths for the forward and reverse transitions are not the same, what differs from previous findings of Ali and Seshadri [1], who stated that there were no changes in the pressure drop measurements, whether the spiral was fed on the inside or the outside.

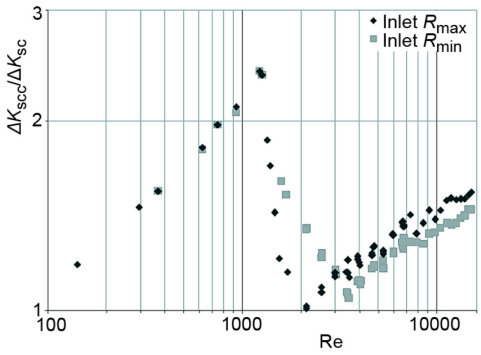

Figure 6. Prediction of critical Reynolds numbers

The method of White [28] and Adler [29], originally proposed for curved pipes, was used for the location of critical Reynolds numbers. This originally consists of plotting the ratio $\Delta P_{scc}/\Delta P_{sc}$, *vs.* Reynolds number, where ΔP_{scc} and ΔP_{sc} are the pressure drops at the same Reynolds number in a corrugated spiral coil and a corrugated straight tube, respectively, of equal length and cross-sectional diameter. In this case the ratio K_{scc}/K_{sc} *vs.* Reynolds number was plotted (fig. 6), where loss coefficient for straight tube was calculated from eqs. (10)-(13).

There are two critical Reynolds numbers in a particular spiral, one where turbulence has set only in the outer turns with lowest curvature ratio (corresponds to first break points in fig. 6), and the other, when the inertia forces, even in the innermost turns with highest curvature ratio, are sufficient to overcome the damping effect of the secondary flows (corresponds to second break points in fig. 6). Hence, the first break corresponds to laminar flow everywhere except in a small region in the outer turns and the second break corresponds to the flow becoming turbulent everywhere. At the approach of the first critical Reynolds number turbulence appears at the maximum radius point of the coil, and spreads to greater length with the further increase in Reynolds number. The first critical Reynolds number in corrugated Archimedean spiral, whether it was fed on the inside or the outside, corresponds to the value of the critical Reynolds number in straight corrugated tube (Re ≈ 1300), and remains unaffected by the direction of the flow. The second critical Reynolds number is obtained by adding corrugation parameters, corrugation depth, and corrugation pitch, to corresponding equation of Ali and Seshadri [1]:

– inflow to outermost spiral turn

$$\mathrm{Re}_{\mathrm{scc\,crit\,I}} = \mathrm{Re}_{\mathrm{sc\,crit}} = 1300 \tag{23}$$

$$\mathrm{Re}_{\mathrm{scc\,crit\,II}} = \mathrm{Re}_{\mathrm{sc\,crit}}\left[1 + 6.25\left(\frac{d}{R_{\min}}\right)^{0.17}\left(\frac{p_{\mathrm{s}}}{R_{\min}}\right)^{0.1}\right]\left(\frac{e}{p_{\mathrm{c}}}\right) \tag{24}$$

– inflow to innermost spiral turn

$$\mathrm{Re}_{\mathrm{scc\,crit\,I}} = \mathrm{Re}_{\mathrm{sc\,crit}} = 1300 \tag{25}$$

$$\mathrm{Re}_{\mathrm{scc\,crit\,II}} = \mathrm{Re}_{\mathrm{sc\,crit}}\left[1 + 6.25\left(\frac{d}{R_{\min}}\right)^{0.17}\left(\frac{p_{\mathrm{s}}}{R_{\min}}\right)^{0.1}\right]\left(\frac{e}{p_{\mathrm{c}}}\right)^{0.6} \tag{26}$$

Equations (23)-(26) are applicable for flows in Archimedean spiral coils with rough walls of the *d type*, typified by closely spaced spanwise ribs with *p/k* less than 5. They cannot

be compared with other equations because, to the best of our knowledge, this has not been reported before. Numerical verification could be very demanding in considered complex geometry, while further experimental verification implies consideration of the whole geometric family of corrugated pipes.

Conclusions

Applications of curved channel and rough surface flow geometries demand the experimental evaluation of the pressure losses. Investigated straight corrugated pipe, before bending it into spiral, characterized by closely spaced narrow lateral grooves of *d type*, behaves as a smooth tube at low Reynolds numbers. Corrugations accelerate transition to critical Reynolds numbers down to 1300. The distribution of the friction factor *f vs.* Reynolds number in the critical and transition regimes duplicates value trends of Nikuradse's results for artificially roughened pipes with uniform sand grains, while in the fully rough regime, at higher Reynolds numbers, friction factor tends asymptotically to some constant value. The validity of obtained correlations for the friction factor in straight corrugated pipe can be guaranteed only for pipes having geometric similarity with specified geometrical configuration.

The pressure drop measurements show that the hydrodynamics of the Archimedean spiral tube with transverse corrugations depends on the direction of the flow. In the laminar and transition flow regime, an innermost fed spiral shows higher pressure drops than the outermost fed spiral, but in the turbulent flow regimes, the reverse is true. This is probably due to the influence of inertial forces on developing complex secondary flow in such geometry. In turbulent flow regimes, pressure loss monotonically increases with increase of Reynolds number. The coiling effect factor, $\Delta P_{scc}/\Delta P_{sc}$, shows that the first critical Reynolds number remains unaffected by the direction of the flow and equals the critical Reynolds number of the straight corrugated pipe, while the second critical Reynolds number depends on the direction of the flow through the spiral coil. The pressure drop change with the direction of the flow in the transition region indicates that the transition lengths for the forward and reverse transition are not the same. The characterizing geometrical groups which take into account all the geometrical parameters of Archimedean spiral and corrugated pipe has been obtained. Modifications of the coefficients and powers of amended equations for Archimedean spiral smooth tube give satisfactory correlations.

Acknowledgment

This investigation was part of project III 42006 of Integral and Interdisciplinary investigations of the Republic of Serbia and project TR 33015 of Technological Development of the Republic of Serbia. We would like to thank the Ministry of Education, Science, and Technological Development of the Republic of Serbia for support during this investigation.

Nomenclature

D_{av} – average spiral coil diameter [= $(D_{min}+ D_{max})/2$], [m]
d – minimum internal diameter, [m m]
d_e – maximum external diameter, [mm]
d_o – maximum internal diameter, [mm]
Eu – Euler number (= $\Delta P/\rho V^2$), [–]
e – corrugation depth [$e = (d_o – d)/2$], [mm]
f – Darcy friction factor, [–]
f_{sc} – Darcy friction factor for straight corrugated tube, [–]
f_{scs} – Darcy friction factor for smooth spiral coil, [–]
f_{ss} – Darcy friction factor for straight smooth tube, [–]
K – loss coefficient, [–]
K_{sc} – loss coefficient of corrugated straight tube, [–]

K_{scc} – loss coefficient of corrugated spiral coil, [–]
K_{scs} – loss coefficient of smooth spiral coil, [–]
k – roughness height, [mm]
L_e – length of entrance and exit sections, [m]
L_{sc} – length of tested section of corrug. straight pipe, [m]
L_{scc} – length of tested section of corrugated spiral coil, [m]
L_{scs} – length of smooth spiral coil, [m]
n – number of coil turns, [–]
p – pitch, [mm]
p_c – corrugation pitch, [mm]
p_s – spiral coil pitch, [mm]
ΔP_{sc} – pressure drop in corrugated straight tube, [Pa]
ΔP_{scc} – pressure drop in corrugated spiral coil, [Pa]
ΔP_{scs} – pressure drop in smooth spiral coil, [Pa]
Re – Reynolds number (=$Vd\rho/\mu$), [–]
$Re_{sc\ crit}$ – critical Reynolds number of the corrugated straight tube, [–]
$Re_{scc\ crit\ I}$ – first critical Reynolds number of the corrugated spiral coil, [–]
$Re_{scc\ crit\ II}$ – second critical Reynolds number of the corrugated spiral coil, [–]
R_{max} – maximum radius of spiral coil, [mm]
R_{min} – minimum radius of coil, [mm]
S – wall thickness, [mm]
T – thermodynamic temperature, [K]
t – temperature, [°C]
V – mean axial velocity, [ms^{-1}]

Greek symbols

μ – dynamic viscosity, [Pa·s]
ρ – density of fluid, [kgm^{-3}]

References

[1] Ali, S., Seshadri, C., Pressure Drop in Archimedean Spiral Tubes, *Industrial and Engineering Chemistry Process Design and Development*, *10* (1971), 3, pp. 328-332
[2] Naphon, P., Wongwises, S., A Review of Flow and Heat Transfer Characteristics in Curved Tubes, *Renewable and Sustainable Energy Reviews, 10* (2006), 5, pp. 463-490
[3] Naphon, P., Wongwises, S., An Experimental Study on the In-Tube Convective Heat Transfer Coefficients in a Spiral Coil Heat Exchanger, *International Communications in Heat and Mass Transfer*, *29* (2002), 6, pp. 797-809
[4] Naphon, P., Suwagrai, J., Effect of Curvature Ratios on the Heat Transfer and Flow Developments in the Horizontal Spirally Coiled Tubes, *International Journal of Heat and Mass Transfer*, *50* (2007), 3-4, pp. 444-451
[5] Yoo, G., *et al.*, Fluid Flow and Heat Transfer of Spiral Coiled Tube: Effect of Reynolds Number and Curvature Ratio, *Journal of Central South University, 19* (2012), 2, pp. 471-476
[6] Bowman, A., Park, H., CFD Study on Laminar Flow Pressure Drop and Heat Transfer Characteristics in Toroidal and Spiral Coil System, *Proceedings*, ASME 2004 International Mechanical Engineering Congress and Exposition, Anaheim, Cal., USA, 2004
[7] Altac, Z., Altun, O., Hydrodynamically and Thermally Developing Laminar Flow in Spiral Coil Tubes, *International Journal of Thermal Sciences*, *77* (2014), Mar., pp. 96-107
[8] Perry, A., *et al.*, Rough Wall Turbulent Boundary Layers, *Journal of Fluid Mechanics, 37* (1969), 2, pp. 383-413
[9] Tani, J., Turbulent Boundary Layer Development over Rough Surfaces, *Perspectives in Turbulence Studies* (Eds. U. Meier, P. Bradshaw), Springer Verlag, Tokio, Japan, 1987, pp 223-249
[10] Jaiman, R., *et al.*, CFD Modeling of Corrugated Flexible Pipe, *Proceedings*, 29th International Conference on Offshore Mechanics and Arctic Engineering, Shanghai, China, 2010
[11] Pisarenko, M., *et al.*, Friction Factor Estimation for Turbulent Flows in Corrugated Pipes with Rough Walls, *Journal of Offshore Mechanics and Arctic Engineering, 133* (2011), 1, pp. 011101-1-10
[12] Vijiapurapu, S., Cui, J., Simulation of Turbulent Flow in a Ribbed Pipe Using Large Eddy Simulation, *Numerical Heat Transfer, Part A, 51* (2007), 12, pp. 1137-1165
[13] Bernhard, D., Hsieh, C., Pressure Drop in Corrugated Pipes, *Journal of Fluids Engineering, 118* (1996), 2, pp. 409-410
[14] Taylor, J. *et al.*, Characterization of the Effect of Surface Roughness and Texture on Fluid Flow – Past, Present and Future, *International Journal of Thermal Sciences, 45* (2006), 10, pp. 962–968
[15] ***, Pliable Corrugated Stainless Steel Resistant to Corrosion CSST Tubes for Plumbing, Heating Systems and Thermal Solar Plants, Eurotis S.l.r., Italy, http://www.eurotis.it.
[16] ***, Revised Release on the IAPWS Formulation 1995 for the Thermodynamic Properties of Ordinary Water Substance for General and Scientific Use, 2009, IAPWS, http://www.iapws.org.

[17] Kline, S., McClintok, F., Describing Uncertainties in Single-Sample Experiments, *Mechanical Engineering, 75* (1953), 1, pp. 3-8
[18] Hetsroni, G., *et al.*, Micro-Channels: Reality and Myth, *Journal of Fluids Engineering, 133* (2011), 12, pp 121202-1-14
[19] Kandlikar, S., *et al.*, Characterization of Surface Roughness Effects on Pressure Drop in Single-phase Flow in Minichannels, *Physics of Fluids, 17* (2005), 5, pp. 100606-1-11
[20] Colebrook, C., Turbulent Flow in Pipes, with Particular Reference to the Transition Region between the Smooth and Rough Pipe Laws, *Journal of the Institution of Civil Engineers*, *11* (1939), 4, pp. 133-156
[21] Moody, L., Friction Factors for Pipe Flow, *Transactions of the American Society of Mechanical Engineers*, *66* (1944), pp. 671-684
[22] Fang, X., *et al.*, New Correlations of Single-Phase Friction Factor for Turbulent Pipe Flow and Evaluation of Existing Single-phase Friction Factor Correlations, *Nuclear Engineering and Design, 241* (2011), 3, pp. 897-902
[23] Churchill, S., Friction Factor Equations Spans All Fluid Flow Ranges, *Chemical Engineering, 84* (1977), 24, pp. 91-102
[24] Schroeder, D., *A Tutorial on Pipe Flow Equations*, Stoner Associates, Inc., Carlisle, Penn., USA, 2001
[25] Chen, N., An Explicit Equation for Friction Factor in Pipe, *Industrial and Engineering Chemistry Fundamentals, 18* (1979), 3, pp. 296-297
[26] Kubair, V., Kuloor, N., Flow of Newtonian Fluids in Archimedean Spiral Tube Coils: Correlation of the Laminar, Transition and Turbulent Flows, *Indian Journal of Technology*, *4* (1966), 1, pp. 3-8
[27] Rennels, D., Hudson, H., *Pipe Flow – A Practical and Comprehensive Guide*, John Wiley and Sons, Hoboken, N. J., USA, 2012
[28] White, C., Streamline Flow Trough Curved Pipes, *Proceedings of the Royal* Society, *Ser. A, 123* (1929), 792, pp. 645-663
[29] Adler, M., Flow in Curved Pipes (in German), *Journal of Applied Mathematics and Mechanics, 14* (1934), 5, pp. 257-275

Paper submitted: January 18, 2015
Paper revised: July 28, 2015
Paper accepted: November 22, 2015